Electrocoloration in $SrTiO_3$: Vacancy Drift and Oxidation-Reduction of Transition Metals

Joseph Blanc and David L. Staebler
RCA Laboratories, Princeton, New Jersey 08540
(Received 3 June 1971)

Application of dc electric fields, at temperatures of ~100 to ~325 °C, to samples of $SrTiO_3$ doped with transition metals leads to the appearance of colored regions, characteristic of reduced material at the cathode and oxidized material at the anode. This process is reversible upon reversal of the polarity of the applied field. We have measured the space and time dependencies of the optical and electrical properties of such samples of $SrTiO_3$. All of the phenomena can be quantitatively understood in terms of a simple model, whose major ingredient is the drift of doubly positive oxygen vacancies across regions of high electric field, with accompanying oxidation and reduction of stationary transition-metal ions. Interpretation of our data yields quantitative estimates for the mobility of oxygen vacancies in this temperature range. For very long times of electrocoloration, the proposed model is inadequate for a quantitative description of the observed phenomena. This limitation is largely due to the formation of unusual oxidation states and complexes whose detailed nature is not yet completely understood.

I. INTRODUCTION

There is, by this time, substantial literature on the photochromic behavior of $SrTiO_3$.[1-6] There also have been a number of publications on time dependences of conductivity in the same material.[7] In addition, there have been scattered reports of coloration induced under applied electric fields both in $SrTiO_3$[8] and $BaTiO_3$.[9] The work we report here probes the correlation between these phenomena and attempts to present a plausible model to explain these in terms of electrical and optical properties of $SrTiO_3$. The present work follows from the preliminary results presented by Faughnan and Kiss.[8]

Since a central part of our explanation involves the dominant role of vacancy motion under applied electric fields, we wish to establish at the outset that in insulating $SrTiO_3$ the dominant conductivity mechanism at room temperature is overwhelmingly likely to be ionic conductivity (through oxygen vacancies) rather than electronic conductivity (through electrons or holes). For electron conduction to dominate, the following ratio must exceed unity:

$$\frac{\sigma\ (\text{electronic})}{\sigma\ (\text{vacancies})} = \frac{n\mu_e}{N_V\mu_V} \ .$$

n is the electron concentration, N_V is the vacancy concentration, and μ is the mobility. μ_e is known[10] to be of the order of 1 $cm^2/V\,sec$; a hazardous but conservative extrapolation of high-temperature diffusion data[11] yields an estimate of $\mu_V \geq 10^{-9}$ $cm^2/V\,sec$ at room temperature. The inequality for σ_V to be dominant can therefore be expressed as $N_V > 10^9\, n$. We now provide a guess at n. From standard semiconductor statistics

$$n = [(N_D - N_A)N_c\, e^{-E/kT}]/N_A \ .$$

We take E, the ionization energy, ~1 eV (see Sec. IV); $(N_D - N_A)/N_A$, the compensation ratio, is equal to 10; N_c, the density of states, $\sim 10^{20}/cm^3$. On these assumptions, $n \simeq 10^{21}\, e^{-40} \simeq 10^4/cm^3$. Therefore, N_V should be more than $10^{13}/cm^3$ for vacancy conductivity to predominate. Although this estimate is likely to be in error by one or two orders of magnitude, we believe it clearly shows the likelihood of ionic conductivity in $SrTiO_3$ containing, as we show later, more than $10^{18}/cm^3$ vacancies. We remark, in passing, that although the appropriate parameters are not known for $BaTiO_3$, they are likely to be similar to those of $SrTiO_3$; the extensive literature on the "aging problem" in ferroelectric $BaTiO_3$[12] seems to have largely ignored experiments that strongly suggest the role of ionic conductivity.[13]

The experiments we describe below show that under controlled conditions of impurity (temperature and applied electric field) very large changes in conductivity and optical absorption can be obtained in $SrTiO_3$. These effects can be easily understood to first order in terms of a simple model. This model is formally analogous to the theory of the preparation of Li-doped Si p-i-n structures,[14] with mobile oxygen vacancies in $SrTiO_3$ playing the role of mobile Li ions in Si. We show that, in $SrTiO_3$, such a process can produce large color changes due to oxidation and reduction of transition-element dopants. These experiments also show a richness and complexity in defect-defect interactions in $SrTiO_3$ which have heretofore been unnoticed; our understanding of these is still imperfect.

In Sec. II, we briefly describe our experimental apparatus. Section III gives a general description

of the phenomenon of electrocoloration in transition-metal-doped $SrTiO_3$. Section IV presents our model with a detailed experimental comparison for a case where the necessary parameters are known. Section V discusses limitations of this model as well as other various kinds of evidence for more complex defect behavior than is handled by this model.

II. EXPERIMENTAL

Materials. Single crystals of transition-metal-doped $SrTiO_3$ were purchased from National Lead Company. Mass spectrographic and atomic absorption analyses on samples used by us, or samples similar to ours, were performed by Herrington and Whittaker of our laboratories. These analyses showed that the actual concentrations of added impurities were typically a factor of 5 lower than those quoted by the supplier. Typical dimensions of the parallelepiped used in our experiments were 15 mm long, 3 mm wide, and 1 mm or less thick.

Voltage and current control. A Kepco model BHK 2000 – 0.1 M was used either in constant voltage or constant current modes. A feedback circuit incorporating a Keithly 610A was built for use in conjunction with the Kepco to control currents less than 10^{-3} A. Voltage (at constant current) or current (at constant voltage) could be recorded on a Varian recorder.

Resistance and potential-profile measurements. Measurements were made by a "four-point" probe method, in which the voltage drop at known current across a portion of the crystal was measured by a Keithly 602 electrometer.

Electrical contacts. Electrodes were evaporated aluminum, as were thin contacting strips used in the four-point resistance measurements. Profile measurements were made using a micromanipulator equipped with tungsten points. Both aluminum and tungsten proved to make contacts with "stoichiometric" and reduced $SrTiO_3$ whose resistance was much less than bulk resistance; for oxidized $SrTiO_3$, these contact resistances were not small (see Sec. IV). We attempted to overcome this by copper, silver, and graphite (Dag) contacts; all these gave the same qualitative behavior. In addition, there was visible evidence (in the form of small black spots) that silver migrated into the crystal under the influence of applied electric fields.

Optical measurements. Absorption measurements from the band edge (~3900 Å) to 17 000 Å were made on a Cary model 14R with appropriate blanks and base line corrections.

Temperature control. Samples with appropriate contacts were placed on a small hot plate, whose temperature was regulated to better than $\frac{1}{2}$ °C through the use of a controller designed by Hook of these laboratories. After we had found that the effects we were investigating are independent of ambient atmosphere, this heating arrangement was placed within a Plexiglas enclosure which both prevented shock hazard and guaranteed essentially isothermal conditions.

III. GENERAL FEATURES OF "ELECTROCHROMISM" IN $SrTiO_3$

It is known from the work of Faughnan[1–4] and others[5,6] that transition metals on Ti sites can exist in several formal oxidation states, e.g., Mo^{+5}, Mo^{+6} or Ni^{+1}, Ni^{+2}, Ni^{+3}, and that such ions can be changed from one charge state to another by oxidation or reduction heat treatments. It is also characteristic that one charge state of the ion (i.e., Ni^{+2}) gives rise to no appreciable absorption in the visible or near infrared portions of the spectrum. A sample doped with transition metal can be oxidized or reduced, as appropriate, to bring the sample to this "colorless" state. This colorless state of the crystal has been our usual starting point for the observation of electrochromism.

If an electric field is applied to such a sample at temperatures above 130 °C either in air, vacuum, or inert atmosphere, the region around the *negative* electrode develops a color characteristic of the *reduced* form of the transition metal; next to the positive electrode, color characteristic of the *oxidized* form is seen. These two color fronts move towards each other, with rather diffuse and jagged boundaries, until they eliminate the intermediate colorless region. Having met, the boundary formed between the oxidized and reduced regions is stationary (on a time scale which will be made precise below) so that further application of electric field leads to no observable changes. Reversal of the field polarity leads to a retreat of the colored regions from each other, with sharply defined smooth boundaries, leaving a well-defined colorless region in between. If this reverse process is allowed to continue, the colored regions are eventually "swallowed" up in the contacts and then reappear as reverse coloration begins. This process of coloring and uncoloring may apparently be carried on indefinitely.

This description of the qualitative features of electrochromism in $SrTiO_3$ is adequate only for times shorter than that required to move a vacancy from one contact to the other, i.e., a time shorter than $t \simeq 2eN_V \times$ sample volume$/I$ (e is the electronic charge, N_V is the concentration of doubly positive oxygen vacancies, and I is the current). For $N_V \simeq 10^{18}/\text{cm}^3$, volume of $\sim 10^{-2}$ cm^3, and $I = 10^{-6}$ A, then $t \simeq 2000$ sec. Our quantitative analyses will be restricted to this "short-time" domain. We qualitatively discuss behavior in the "long-time"

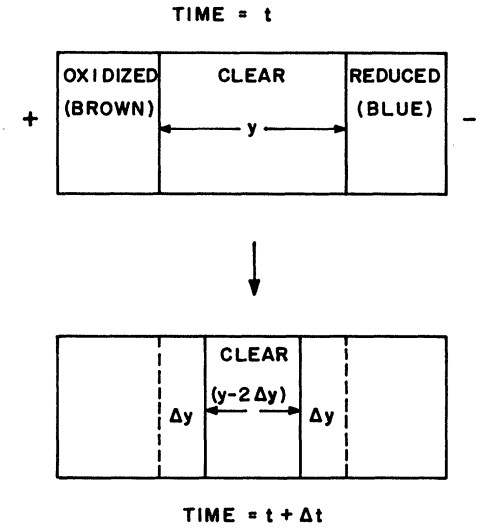

FIG. 1. Schematic sketch of proposed model. The clear region is much lower conductivity than the two colored regions, so that at any instant the applied voltage falls only across "y." Doubly positive oxygen vacancies thus tend to move towards the right-hand side, decreasing the width of the clear region.

domain in Sec. V of this paper.

The coloration features listed above have been found by us to hold for all transition metals we have studied: Ni, Fe, Co, and Mo, singly or multiply doped. However, for the sake of clarity and brevity, detailed results will be given only for $SrTiO_3$ doped with Ni and Mo. This choice has been made because the necessary charge balance equations will have a more readily interpretable form in the case of double doping, and because we have been able to establish (in work to be reported separately[15]) that the optical absorption due to "reduced" Ni has the symmetry required by the "axial" $(Ni^{3+} - V_O^{0})$ center observed by electron-spin resonance.[1,6]

IV. THE MODEL AND SOME EXPERIMENTAL CONFIRMATIONS

In order to present our results succinctly, we first introduce our model for general electrochromic behavior. We assume, first, based on the optical data discussed above, that the electrochromically induced color changes are due to oxygen vacancy motion in the crystal. Next we assume that the conductivities of both oxidized and reduced regions are very much larger than that of the colorless region, which has conductivity due, at least in part, to the motion of doubly positive vacancies. Now consider a sample at an intermediate stage of coloration as in Fig. 1. At time t, the width of the clear region is y, while a current I is applied with voltage V. Because the conductivities of the colored regions are high, all of the applied voltage falls across the clear region. The resulting field will move vacancies to the right, away from the "clear"-oxidized boundary. After a time dt, the oxidized region will have increased its length by

$$dy = \mu_V E\, dt = (\mu_V V/y)\, dt \ .$$

We assume here that no vacancies remain in the oxidized region. Over the same time period, vacancies will have arrived at the "clear"-reduced interface, increasing the length of the reduced region. In order to simplify numerical factors, we assume that the two colored regions increase their length by the same amount. The clear region has decreased its length by $2dy$ during this time interval, or the total change in y is $2\mu_V V\, dt/y$. An entirely analogous argument can be made for the opposite polarity. Therefore, the initial equation for our model is

$$-\frac{dy}{dt} = \frac{2\mu_V V}{y} \ . \tag{1}$$

Assuming Ohmic behavior across the clear region, $V = Iy/A\sigma$, where I is the current, A is the cross-sectional area, and σ is the conductivity of the clear region,

$$-\frac{dy}{dt} = \frac{2\mu_V I}{A\sigma} \ . \tag{2}$$

The conductivity due to vacancies is $\sigma_V = 2eN_V\mu_V$, so that Eq. (2) can be written

$$-\frac{dy}{dt} = \left(\frac{\sigma_V}{\sigma}\right)\left(\frac{I}{A}\right)\left(\frac{1}{eN_V}\right) \ . \tag{3}$$

These equations show that at constant applied current, the clear region opens (or closes) at a constant rate, proportional to the current.

We note, for future purposes, that if the total conductivity is all due to vacancies, $\sigma_V = \sigma$, then dy/dt at constant current should be *independent of temperature*. This is not an assumption of the model, and it therefore permits an evaluation of the relative importance of electronic vs vacancy conductions. We note also that, *if* $\sigma_V = \sigma$, we may obtain an estimate of the vacancy concentration in the clear region from experimentally determined quantities.

Constant current conditions also require that the applied voltage change linearly with time. That is,

$$\left(\frac{\partial V}{\partial t}\right)_I = \left(\frac{I}{A\sigma}\right)\left(\frac{dy}{dt}\right) = -\left(\frac{I}{A\sigma}\right)^2\left(\frac{\sigma_V}{eN_V}\right) \ . \tag{4}$$

From the first equality of Eq. (4), it can be seen that, if the model is substantially correct, the conductivity of the clear region can be obtained, be it of ionic or electronic origin, by measurements of both $(\partial V/\partial t)_I$ and dy/dt. The second equality indi-

cates that $(\partial V/\partial t)_I$ should be proportional to the square of the current.

It is important to point out that the above equations are directly relevant to situations where the boundaries remain smooth and well defined. As we mentioned in Sec. III, this is observed only during "uncoloration." Such a boundary property is consistent with the proposed conductivity properties which require that most of the voltage appear across the clear region. For this condition, a boundary with sharp points extending into the clear region becomes smoothed out during uncoloration by the high driving field at these points. During forward coloration, however, this effect emphasizes any irregularity to produce a jagged or hazy boundary. Because of this, quantitative measurements of boundary motion are restricted to experiments during which the clear region becomes wider.

We now present, in detail, data for one crystal which was doped with $\sim 4\times10^{18}$ Ni/cm^3, 4×10^{18} Mo/cm^3, and 5×10^{18} Al/cm^3. While this may seem a needlessly complicated case to examine, it has the great advantage that the optical absorption features can be definitely ascribed, so that significant checks of internal consistency are available. The aluminum present in this and other analogous samples doped with Fe, Mo was added for reasons of charge compensation. We have found no evidence for any optical absorption due to Al in any form nor any evidence to indicate that it changes its oxidation state from the normal Al^{+3}.

Absorption spectra obtained at room temperature from one sample of this crystal are shown in Fig. 2. The data shown for the "brown" and "blue" curves were obtained after heating the sample to 300 °C, applying a current until the brown color emanating from the positive electrode and the blue color coming from the negative electrode just touched, and then switching off the current and cooling the sample. The clear region was then obtained by reheating and reversing the polarity until the clear region was about $\frac{1}{3}$ of the sample. The blue region is dominated by an absorption at about 6500 Å, shown by Faughnan[1] to be in one-to-one correspondence with Mo^{+5} in the lattice. There is a small shoulder at 4800 Å associated with a (Ni^{+3}-vacancy) complex. In the brown region there is only a very strong unstructured absorption whose intensity Faughnan has shown to be in correspondence with Ni^{+3} in the lattice. In the clear region, there is very little absorption in the visible and we may safely conclude that there is little Mo^{+5}, "Ni^{+1}", or Ni^{+3} present here.

The conductivities of these three regions, plotted as $\log\sigma$ vs $1/T$, are shown in Fig. 3, and it can be seen that over the whole temperature interval covered, σ(clear) is indeed much lower than σ(brown) and σ(blue), thus directly validating one of the principal assumptions of the primitive model.

Figure 4 shows a plot of clear-region volume, the product of the cross-sectional area A and the width y, at a current of 10^{-6} Å at nominal temperatures of 200, 250, and 300 °C. (The true temperatures of the sample were undoubtedly slightly lower as the use of camera and microscope in these experiments necessitated the removal of the Plexiglas enclosure.) We see that y is indeed a linear function of time and that dy/dt is independent of

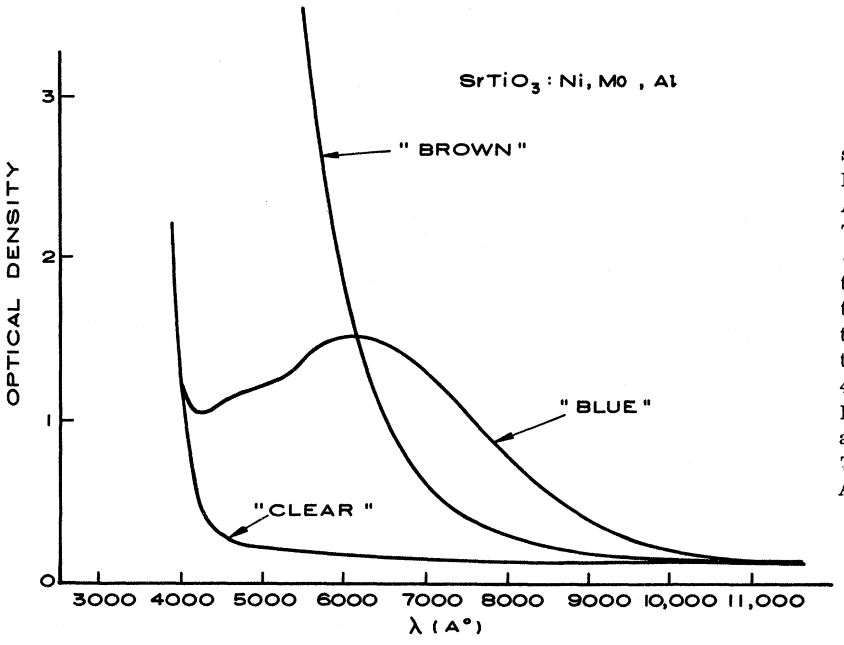

FIG. 2. Absorption spectrum of a sample of $SrTiO_3$ containing 4×10^{18} Ni/cm^3, 4×10^{18} Mo/cm^3, and 5×10^{18} Al/cm^3. The path length was 0.08 cm. The brown absorption corresponds to electro-oxidation and is due entirely to Ni^{+3} on Ti sites. The blue absorption corresponds to electroreduction; the prominent band at $\sim$6500 Å is due to Mo^{+5} on Ti sites; the shoulder at 4800 Å is due to a (Ni^{+2}-V^0) complex. In the clear region, the Ni is present as Ni^{+2}; the Mo is present as Mo^{+6}. There is no absorption ascribable to Al.

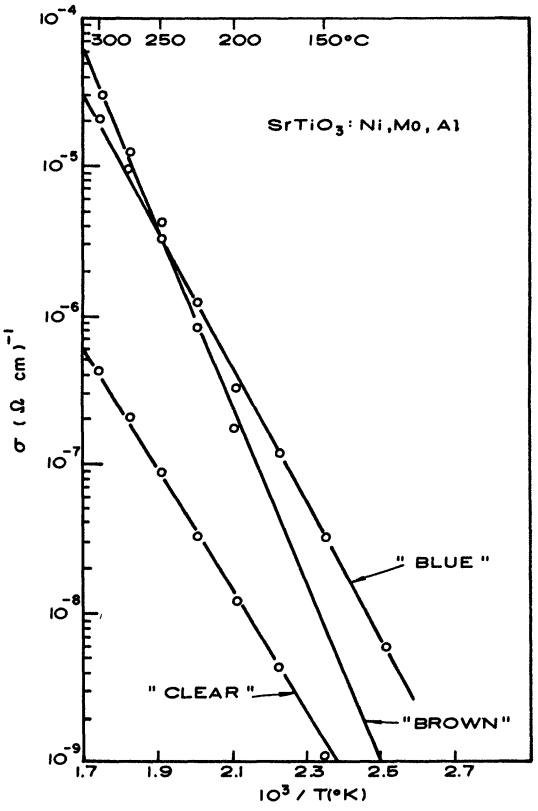

FIG. 3. Conductivities of $SrTiO_3$ doped with Ni, Mo, and Al. Same sample as in Fig. 2.

temperature. The first point supports Eq. (3); the second implies on our model that essentially all the conductivity is via vacancies. Figure 5 shows a plot of voltage V vs time under the same conditions of temperature and current as Fig. 4. The voltage does change linearly with time, the slopes being markedly dependent on temperature, thus supporting Eq. (4). We have also confirmed the fact expected from (4) that $(\partial V/\partial t)_I$ is proportional to I^2. These data are not quoted here, as they are essentially redundant, and no further physical parameters can be extracted from them.

In view of the agreement between the electrochromic experimental data, and Eqs. (3) and (4), we now solve Eq. (4) for σ:

$$\sigma = \left(\frac{I}{A}\right)\left(\frac{dy}{dt}\right)\left(\frac{\partial V}{\partial t}\right)^{-1} .$$

Figure 6 shows the clear-region conductivities so calculated. The maximum deviation between calculated and measured conductivities is ~30% at 300 °C. In view of the fact, previously noted, that the calculated conductivities were obtained under conditions where the sample was slightly cooler than nominal, we consider the agreement as essentially complete.

Since there is such substantial agreement between the predictions of the model and our measurements of electrical properties, we conclude that it is essentially correct in its physical content. In particular, we make the important physical conclusion that electrical transport in the clear region of electrochromic $SrTiO_3$ occurs principally via motion of oxygen vacancies. This now allows us to estimate the vacancy concentration via Eq. (3) and to compare this estimate with concentration estimates available from known impurity concentrations and optical data.

From Eq. (3) we obtain with $\sigma = \sigma_V$ the vacancy concentration in the colorless region, $N_V = 2.3 \times 10^{18}/\text{cm}^3$. This estimate can be checked by knowledge of the impurity concentrations and ap-

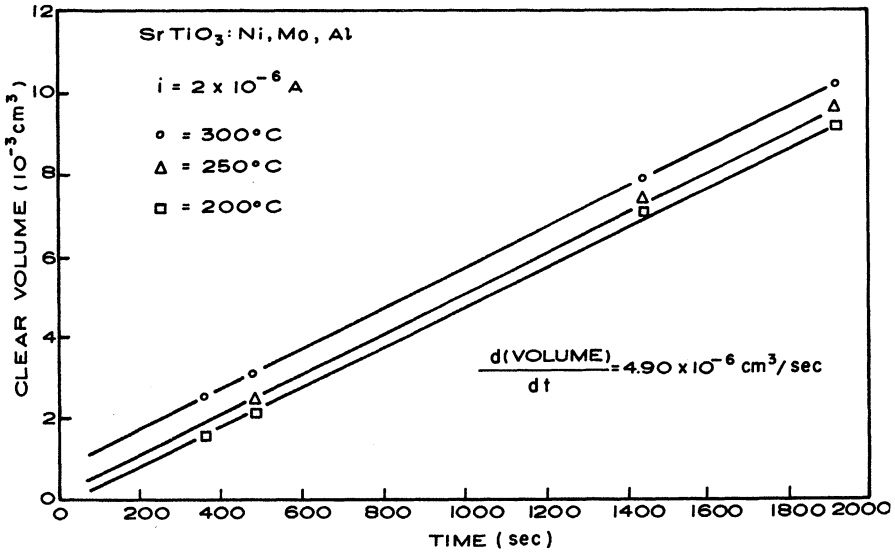

FIG. 4. Increase of clear volume with time for doped sample of $SrTiO_3$ at constant current for three temperatures. The slopes are temperature independent. Sample cross section $\simeq 4.7 \times 10^{-2}\text{cm}^2$.

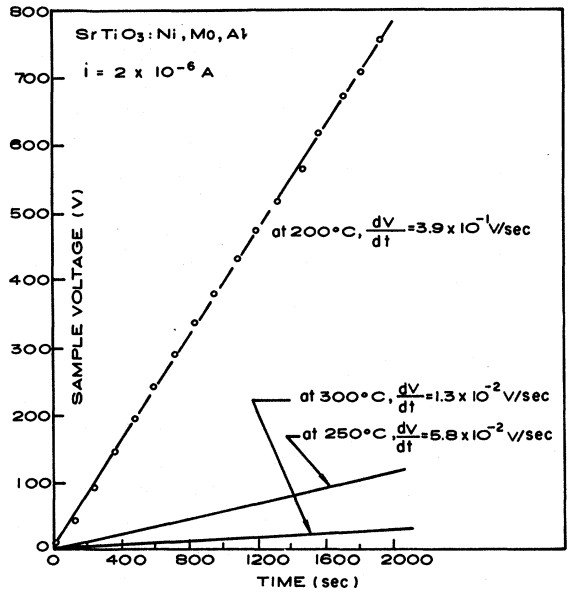

FIG. 5. Increase of total sample voltage with time at constant current. Data points are shown with the uppermost curve to show the excellent linearity of these data.

propriate charge neutrality relations. The impurity concentrations given by chemical analysis are $N_{Mo}=4\times10^{18}/cm^3$, $N_{Ni}=4\times10^{18}/cm^3$, and $N_{Al}=5\times10^{18}/cm^3$. We can, by use of Faughnan's oscillator strength[1] for Mo^{+5} and Ni^{+3} and the data of Fig. 2, obtain independent estimates; these are $N_{Mo}=3\times10^{18}/cm^3$ and $N_{Ni}=3\times10^{18}/cm^3$. In the clear region, Mo is present as Mo^{+6}, Ni as Ni^{+2}, and Al as Al^{+3}. The charge neutrality equation (with charge counted as difference from Ti^{+4}) is

$$2N_V = 2N_{Ni} + N_{Al} - 2N_{Mo} . \quad (5)$$

We thus obtain

$$N_V \simeq \tfrac{1}{2}N_{Al} \simeq 2.5\times10^{18}/cm^3 ,$$

in excellent agreement with the earlier estimate based on our analysis of conductivity.

We can obtain a final estimate on the internal consistency of this calculation by observing that on the oxidized side (no vacancies, Mo as Mo^{+6}, Ni as Ni^{+3})

$$2N_{Mo} = N_{Ni} + N_{Al} , \quad (6)$$

and by subtracting Eq. (6) from Eq. (5) we obtain

$$2N_V = N_{Ni} . \quad (7)$$

Equation (7) yields $N_V \simeq 2.0\times10^{18}/cm^3$ from the chemical data and $1.5\times10^{18}/cm^3$ from the optical experiment. The vacancy concentration in the colorless region is thus

$$1.5\times10^{18}/cm^3 \leq N_V \leq 2.5\times10^{18}/cm^3 .$$

The vacancy mobility in this sample is therefore $\sim 5.5\times10^{-7}$ cm^2/V sec at 300 °C and $\sim 1.5\times10^{-8}$ cm^2/V sec at 200 °C. By similar arguments, which we do not reproduce here, the total vacancy concentration on the *reduced* side is calculated to be $\sim 4.3\times10^{18}/cm^3$, i.e., about twice that in the colorless region, as expected from the model.

In spite of the minor ambiguities encountered in the analysis for vacancy and impurity concentrations, we believe that the ability of the primitive model to give such excellent agreement shows that the primary physical effect involved in the electrochromic behavior is the electric-field-driven motion of oxygen vacancies.

We have not, up to now, attempted to present a rationale for the observation that both oxidized and reduced regions are of very much higher conductivity than the clear regions. The simplest plausible explanation of these observations is that the effect is analogous to formation of the well-known Li-drifted *p-i-n* junctions,[14] where application of reverse bias yields a precisely electronically compensated region in between low-resistivity electronically conducting ends. Direct supporting evidence for the existence of *p* and *n* regions separated by a higher-resistance region is available from voltage profiles on these electrocolored samples. Figure 7 shows such a profile in forward bias at a temperature of 250 °C. (These data are available only with forward bias and in the long-time regime because, on the time scale necessary to obtain the points and with the desired accuracy, we had to use "high" currents; in the reverse direction, this

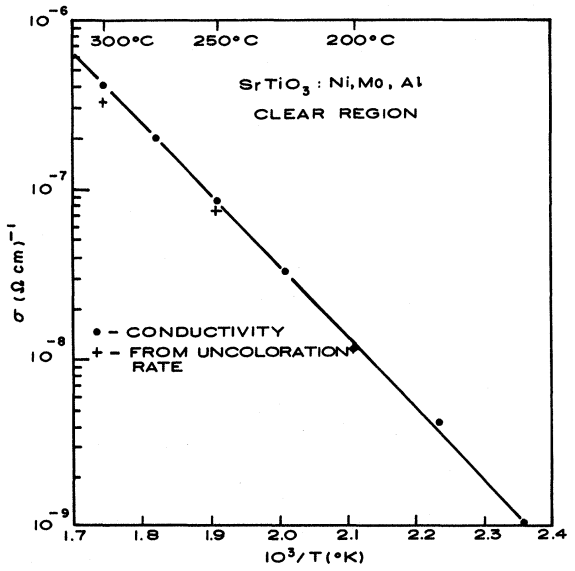

FIG. 6. Test of adequacy of the model. The calculated points (+) are obtained from Eq. (4) and the data of Figs. 5 and 6; the measured points are reproduced from Fig. 3.

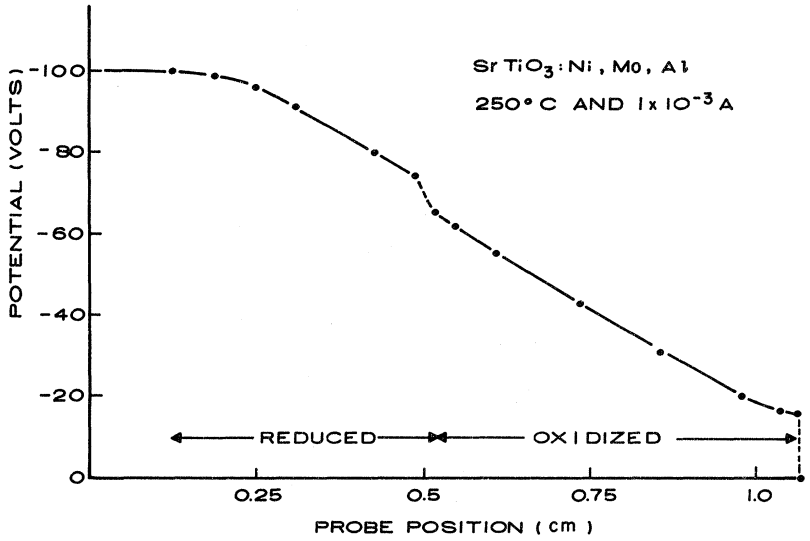

FIG. 7. Potential profile of electrocolored sample. The discontinuity at the oxidized Al contact is interpreted in the text as evidence for p-type conduction in the oxidized region of the crystal.

leads to very rapid disappearance of the coloration.) We focus attention on the regions near the contacts. Near the negative contact, the potential is smooth, but slightly nonlinear; at the positive contact, within the spatial resolution of our probe, there is a discontinuity of ~16 V. Carnes and Goodman[16] have shown that In and Mg make low-resistance contact to n-type $SrTiO_3$. Since the work function of our contact Al is intermediate to the former two metals, we expect that Al should be Ohmic as well. We thus conclude that the reduced region of the crystals is n type, as is, of course, consistent with the observation that highly reduced $SrTiO_3$ is highly n type. Now, a contact that is Ohmic for electron injection into the conduction band should be blocking for hole injection into the valence band. We thus presume that at the onset of coloration no holes are injected and a depletion layer is formed when oxygen vacancies drift away from the anode. When this layer becomes wide enough, it could support a field sufficiently high to induce injection of *holes* over the barrier. Thereafter, subsequent vacancy depletion is charge compensated by injected holes, leaving a depletion layer of constant thickness. We can show that for such a depletion layer the field at the contact is given by

$$E \simeq 10^{-4}(2VN)^{1/2}\ (\mathrm{V/cm})\,,$$

where V is the voltage drop across the barrier and N is the initial concentration of doubly charged vacancies. For the sample shown in Fig. 7, $2N \simeq 5\times10^{18}/\mathrm{cm}^{-3}$ and $V \simeq 16$ V, so that $E \sim 10^6$ V/cm, a field expected to be large enough for hole injection.[17] The thickness of the layer should be $\sim 3\times10^{-5}$ cm, well below our resolution. These considerations show the consistency of viewing the oxidized region as p type and the reduced region as n type. [We note that if the limiting factor were the blocking of *ion* flow at the anode, we would expect much *wider* depletion regions (see Williams[13]).]

V. LIMITATION OF MODEL

The validity of our model has certain intrinsic limits. Two of these are temperature limits; a third is our restriction to "short" times. We discuss the temperature effects briefly, and focus more attention on the behavior at "long" times, which sharply brings out our limited understanding of defects in $SrTiO_3$.

(a) An upper temperature limit arises from the exchange of oxygen between the crystal and the ambient atmosphere. Under these conditions, found above 300 °C, standard thermodynamic forces are prominent rather than electric-field-driven equilibria. This situation is exhibited by a growth of the oxidized region if heated in air, or growth of the reduced region if heated in a vacuum, above ~325 °C. A lower-temperature limit on the applicability of the model is given when the conductivity of the clear region is no larger than those of the colored regions. This always occurs at some temperature lower than that used for "normal" processes since the activation energy for conductivity in the colored regions is invariably larger than that for the clear conductivity. In the limit that the colored conductivity is very small, one can reasonably expect that upon application of a voltage, vacancy drift will continue only until the entire voltage drop occurs at the contacts. Thereafter, there is no tendency for vacancies to drift across the essentially "field-free" colorless region. This is presumably the situation found by Williams[13] in $BaTiO_3$ at room temperature.

(b) We have so far avoided discussions of electrochromic behavior at long times, i.e., times

longer than $(2eN_V V/I)$. In this regime we expect all vacancies should have been swept from the oxidized region into the reduced region; under such circumstances, the model predicts no further vacancy motion. There are at least two intrinsic reasons that such predictions are *not* correct. The first is that on the reduced side there are copious numbers of vacancies, and these can still drift under the small field in this region. The vacancies, therefore, will tend to continue drifting towards the negative electrode. Qualitatively, this should lead to a region near the electrode where the conductivity is dominated by "free" vacancies which are known to be extremely shallow donors in $SrTiO_3$, while the oxidized region slowly increases in size. In the second place, there are circumstances where it is not consistent, even within the primitive model, to assert that all vacancies in the oxidized region can be removed by the electric field. For instance, in samples doped with Ni only, the clear region contains a concentration N of *doubly* positive Ni and a compensating vacancy concentration of N; if the oxidized region contains *triply* positive nickel and local charge neutrality is maintained, the vacancy concentration can decrease only to $N/2$, not to zero. In the sample discussed at length earlier in Sec. IV this effect was nearly compensated by careful counterdoping of Ni by Mo. Both of the above limiting factors can, at the cost of considerable mathematical complexity but little conceptual difficulty, be formally taken into account. We do not do so because the assumption that the only "formal" oxidation states available to Ni are +1, +2, and +3, (Fe +2, +3, and +4) is, in fact, violated at long times, i.e., there is good evidence (shown below) that under prolonged electro-oxidation and reduction, both lower and higher charge states of the transition ions can be formed, as unlikely as these may seem *a priori*.

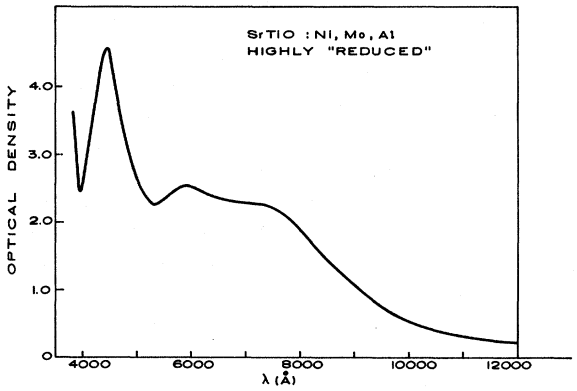

FIG. 8. Absorption spectrum of highly electroreduced sample. Comparison with Fig. 2 shows the new appearance of bands at ~4500 and 5900 Å.

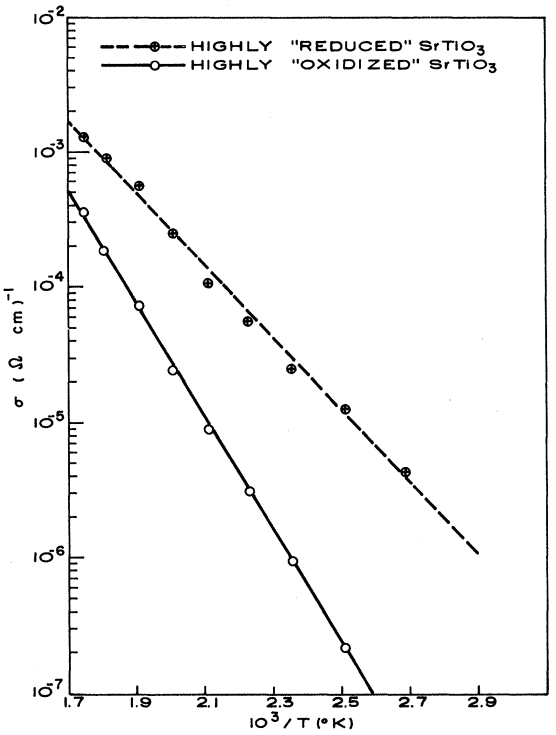

FIG. 9. Conductivities of highly reduced and oxidized samples. Comparison with Fig. 3 shows much higher conductivities and lower activation energies.

The profile data shown in Fig. 7 were, in fact, obtained because of the time necessary to set this experiment up in the long-time regime; that is, after about 3 h with a forward current of 10^{-3} A, or about a factor of 10^3 longer than the short-time limit for this imposed current. After this long time, we find that the oxidized region has enlarged and the properties of both regions are appreciably changed. The reduced region now appears green instead of blue; there is, however, no appreciable change in the absorption of the oxidized region. In addition, the conductivities of both regions are considerably higher than they were in the short-time regime. Figure 8 shows the absorption spectrum of the reduced region, where it can be seen that two features missing from Fig. 2 have appeared: a relatively sharp band at 4500 Å and an unresolved feature at ~5900 Å. In experiments described in another paper,[15] we have shown that the center responsible for these new absorption spectra has the same symmetry as the $(Ni^{+3}\text{-}V^0)$ complex. Figure 9 gives the conductivities of the two regions vs reciprocal temperature; comparison with Fig. 3 shows that at all temperatures the conductivities are much higher, while the activation energies have decreased from ~0.9 to ~0.45 eV on the reduced side and from ~1.25 to ~0.85 eV in the oxidized region. Before proceeding to some

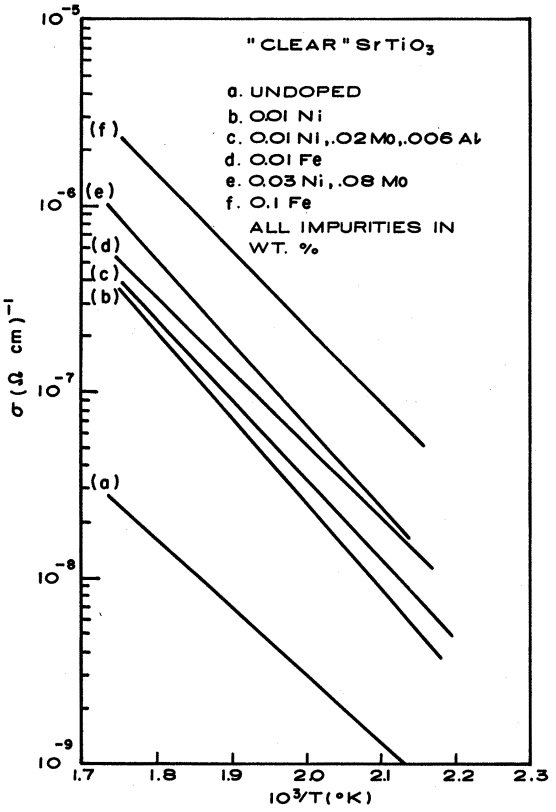

FIG. 10. Examples of conductivities of clear $SrTiO_3$ as a function of impurity content. The concentrations are given as wt% of the oxide.

speculation on the origin of these effects, we emphasize that if such a heavily colored specimen has reverse bias applied, uncoloration proceeds essentially normally; if forward bias is then applied for times which are short, the coloration goes on normally; the oxidized and reduced regions have the *same* electrical and optical properties as they do on initial short-time treatment. We therefore conclude that the observations at long times do not involve gain or loss of matter (i.e., oxygen) from the crystals. The new effects are then presumably due to new "chemical" species formed upon reduction and oxidation.

The reduced behavior is somewhat easier to discuss. As already pointed out, the absorption spectrum shows the same axial symmetry as the (Ni^{+3}-V^0) spectrum; the same spectrum can be induced by hydrogen reduction in $SrTiO_3$ doped with Ni only, except that in these circumstances the crystal is semiconducting with appreciable free-carrier absorption. From these data, it appears reasonable to associate the absorption with a center like (Ni^{+2}-V^0) and the low activation to the ionization process $(Ni^{+2} - V^0) \rightarrow (Ni^{+3} - V^0) + e^-$. We do not, of course, claim to know the actual electron distribution in this complex center.

As we observe no clear-cut new optical absorption associated with the production of oxidized material with activation energy 0.85 eV, the identification is still more speculative. The simplest identification we can propose is a cubic Ni^{+4} on a Ti site. This identification is not entirely without basis, as Müller *et al.*[2] have recently identified the analogous Fe^{+5} by electron-spin resonance in a sample electro-oxidized by us, which did not exhibit any clearly identifiable absorption due to this center.

(c) We now briefly turn our attention to other evidence for complex interactions in $SrTiO_3$. Conductivity vs $1/T$ of several samples of clear $SrTiO_3$ with different dopings is shown in Fig. 10. The activation energies range from about 0.7 to 0.9 eV (16 to 21 kcal/mol); the conductivities are *not* proportional to the impurity content, being of the order of a square root dependence, although this depends on temperature. If these data are analyzed in terms of vacancy drift, the vacancy diffusion coefficients calculated are, below 300 °C, appreciably smaller than those based on an extrapolation of the data of Walters and Grace, the discrepancy increasing with increasing impurity content. Furthermore, our activation energies are very much larger than those obtained by Walters and Grace[11] (~0.2 eV), although they are in the same range as those of Paladino *et al.* in their studies of oxidation kinetics[18] and oxygen diffusion.[19] A suggestive difference between the experiments of Walters and Grace on the one hand, and ours (and probably Paladino's as well) on the other, is that the former workers performed their experiments under conditions where the vacancy concentrations (~10^{20}/cm^3) were in large excess of the impurity content, whereas our studies were performed with vacancy concentrations closely equal to the net acceptor concentrations (i.e., close compensation). This suggests a strong interaction between positively charged vacancies and negatively charged impurities; such interactions would produce higher observed activation energies, lower diffusion coefficients, and a less than linear dependence of vacancy conductivity on vacancy concentration. We do not attempt a quantitative analysis of such a situation because we are not aware of an adequate theory, especially in view of the fact that electron-spin resonance results on transition-metal vacancy pairs shows that these are not simple Coulomb pairs.

ACKNOWLEDGMENTS

We are grateful to G. Latham for his careful and patient assistance in all phases of the experimental work. The phenomena investigated by us

were first observed and brought to our attention by Z. J. Kiss, and the initial quantitative investigations were made by P. Asbeck while he was a summer employee at RCA Laboratories.

[1]B. W. Faughnan, Phys. Rev. (to be published).
[2]K. A. Müller, Th. von Waldkirch, W. Berlinger, and B. W. Faughnan, Solid State Commun. 9, 1097 (1971).
[3]B. W. Faughnan and Z. J. Kiss, IEEE J. Quant. Electron. QE-5, 17 (1969).
[4]B. W. Faughnan and Z. J. Kiss, Phys. Rev. Letters 21, 1331 (1968).
[5]T. C. Ensign and S. E. Stokowski, Phys. Rev. B 1, 2799 (1970).
[6]K. A. Müller, W. Berlinger, and R. S. Rubin, Phys. Rev. 186, 361 (1969).
[7]See R. N. Tredgold, *Space Charge Conduction in Solids* (Elsevier, Amsterdam, 1966).
[8]B. W. Faughnan and Z. J. Kiss (unpublished).
[9]M. S. Kosman and E. V. Bursian, Dokl. Akad. Nuak SSSR 115, 483 (1957) [Sov. Phys. Doklady 2, 354 (1957)].
[10]O. N. Tufte and P. W. Chapman, Phys. Rev. 155, 796 (1967).
[11]L. C. Walters and R. E. Grace, J. Phys. Chem. Solids 28, 239 (1967); 28, 245 (1967).
[12]See R. C. Bradt and G. S. Ansell, J. Am. Ceram. Soc. 52, 192 (1969), for a recent analysis with extensive bibliography.
[13]R. Williams, J. Phys. Chem. Solids 26, 399 (1965).
[14]E. M. Pell, J. Appl. Phys. 31, 291 (1960).
[15]D. L. Staebler and J. Blanc (unpublished).
[16]J. E. Carnes and A. M. Goodman, J. Appl. Phys. 38, 3091 (1967).
[17]M. A. Lampert and P. Mark, *Current Injection in Solids* (Academic, New York, 1970), p. 189.
[18]A. E. Paladino, J. Am. Ceram. Soc. 43, 476 (1965).
[19]A. E. Paladino, L. G. Rubin, and J. S. Waugh, J. Phys. Chem. Solids 26, 391 (1965).

PHYSICAL REVIEW B VOLUME 4, NUMBER 10 15 NOVEMBER 1971

Even-Parity Lattice Resonances and Anharmonicity in KI: Ag^+

R. D. Kirby*†
Department of Physics and Materials Research Laboratory,‡ University of Illinois, Urbana, Illinois 61801
and Laboratory of Atomic and Solid State Physics,§ Cornell University, Ithaca, New York 14850
(Received 6 July 1971)

We report here the observation of four impurity-induced lattice resonances in KI:Ag^+. In addition to the well-known T_{1u} symmetry resonant mode at 17.3 cm^{-1}, we have observed two even-parity resonant modes of A_{1g} and E_g symmetries at 25 and 16.35 cm^{-1}, respectively, and a T_{1u} symmetry gap mode at 86.2 cm^{-1}. The two even-parity modes were detected using far-infrared spectroscopic techniques with the sample in an external electric field. The field induces a strong mixing of the modes of opposite parity and results in large field-induced shifts. The E_g symmetry resonance has also been seen in the Raman spectrum of KI:Ag^+. Two weak and broad absorption lines at 29.8 and 44.4 cm^{-1} are attributed to the E_g+T_{1u} and $A_{1g}+T_{1u}$ combination bands, respectively. These results are interpreted in terms of a model in which the T_{1u} symmetry resonant mode is anharmonically coupled to the even-parity resonances.

I. INTRODUCTION

In recent years there have been a variety of experimental and theoretical investigations of the vibrational properties of substitutional impurities in alkali halides. Thus far, most of the work has been concerned with an understanding of the odd-parity (optically active) local,[1–7] gap,[8,9] and resonant[10–15] modes. However, there can also be impurity-activated resonances with even parity. These modes do not involve any motion of the impurity ion itself, and because of their even parity, will not be optically active in the absence of an external perturbation. To date, even-parity modes have received little attention, apparently because of the difficulties involved in detecting and identifying them.

Both even-parity resonant and gap modes have been observed indirectly as sidebands of the infrared-active *U*-center local mode in KI and KBr.[1–3] The sidebands were made optically active by an anharmonic coupling between the even-parity resonant and gap modes and the odd-parity local mode. In a lattice-dynamical calculation, Gethins *et al.*[16] found it necessary to include rather large force-constant changes between the impurity ion's nearest neighbors and its fourth nearest neighbors (along [100]) to obtain some quantitative agreement with the experimental results of Timusk and Klein.[3]

There is evidence that even-parity resonances have been observed in low-temperature thermal-